Journal of Biotechnology 360 (2022) 45–54

Contents lists available at ScienceDirect

Journal of Biotechnology

journal homepage: www.elsevier.com/locate/jbiotec

# Dynamic modeling of *Rhodospirillum rubrum* PHA production triggered by redox stress during VFA photoheterotrophic assimilations

Paloma Cabecas Segura [a], Ruddy Wattiez [a], Alain Vande Wouwer [b], Baptiste Leroy [a], Laurent Dewasme [b,*]

[a] *Laboratory of Proteomics and Microbiology, University of Mons, 7000 Mons, Belgium*
[b] *Systems, Estimation, Control and Optimization Group (SECO), University of Mons, 7000 Mons, Belgium*

ARTICLE INFO

*Keywords:*
Resource recovery
Wastewater treatment
Parameter estimation
*Rhodospirillum rubrum*
PHA production

ABSTRACT

Polyhydroxyalkanoates (PHA) represent an environmentally friendly alternative to petroleum based plastics for a broad range of applications from packaging to biomedical devices. In the prospect of an industrial PHA production, it is highly valuable to accurately control the incorporation of different repeating units into the polymer, to produce a polyester with specific material characteristics. In this study, we develop macroscopic dynamic models predicting the polymer production and composition when mixtures containing up to four volatile fatty acids (VFA) are used as substrates. These models successfully reproduce the sequential (and preferential) substrate consumption and polymer production/reconsumption patterns, experimentally observed during biomass growth, thanks to simple kinetic structures based on Monod and inhibition factors. These models can serve as a basis for numerical simulation and process analysis, as well as process intensification through model-based optimization and control.

## 1. Introduction

Polyhydroxyalkanoates (PHA) are a family of linear polyester, traditionally accumulated by bacteria as an internal carbon storage compound when a nutrient such as nitrogen or phosphorous is depleted in the environment (Shang et al., 2003). They have risen attention as a potential alternative for petroleum-based plastic as PHA are biodegradable and made from renewable resources while exhibiting mechanical and thermal properties similar to traditional plastic. The wide field of applications of PHA is linked to their exhibited properties, connected to the diversity of their composition (Brandl et al., 1989). The constitutive monomer of the polymer chain or the presence of a comonomer directly impacts the properties of the material (Doi et al., 1995; Gopi et al., 2018; Kale et al., 2015; Kitadokoro et al., 2012; Verlinden et al., 2007). In many different strains, the monomer composition is directly impacted by the carbon sources (Keskin et al., 2017) used to support the growth of the bacteria producing the polymer (Brandl et al., 1991, 1989).

To describe PHA production using volatile fatty acids (VFA) as carbon source, different mathematical models have been developed. Polyhydroxybutyrate (PHB) is the most studied PHA and the first developed models therefore focus on the understanding of its production and degradation process (Beun et al., 2002; Van Aalst-van Leeuwen et al., 1997). Several models have been used to understand PHB accumulation regulation, via the description of an enzyme-structured biomass by taking the increase or decay of a pool of certain enzymes (Salehizadeh and Van Loosdrecht, 2004) or the impact of dissolved oxygen on the microbial conversion of COD into PHB (Third et al., 2003) into consideration. Finally, a process model envisaging the optimization of PHA productivity by mixed microbial culture has been proposed, allowing an accurate description of the process state variables as well as an optimization of the process increasing PHA accumulation (Dias et al., 2005). Some mathematical models have also been developed to predict and control the molecule weight of the produced PHB aiming to improve the physicochemical properties of the polymer (Penloglou et al., 2012). Nonetheless, PHB is a brittle and stiff material that limits its possible application. Other PHA such as poly(hydroxybutyrate-*co*-hydroxyvalerate) (P(HB-*co*-w)) exhibit better mechanical and thermal properties making them suitable for a broader range of applications (Gopi et al., 2018; Kale et al., 2015; Kitadokoro et al., 2012). The developed models have been further broadened to the production of such copolymer using a mixture of acetate and propionate as carbon source (Dias

* Correspondence to: Systems, Estimation, Control and Optimization Group, University of Mons, 31, Boulevard Dolez, 7000 Mons, Belgium.
*E-mail address:* laurent.dewasme@umons.ac.be (L. Dewasme).

https://doi.org/10.1016/j.jbiotec.2022.10.014
Received 21 July 2022; Received in revised form 29 September 2022; Accepted 18 October 2022
Available online 20 October 2022

et al., 2008; Jiang et al., 2011). They consider the conversion of acetate and propionate into acetyl-CoA and propionyl-CoA and their incorporation into the polymer. However, the composition of the waste stream is highly complex and is composed of other fatty acids than acetate and propionate (Dahiya et al., 2015; Jiang et al., 2013; Komemoto et al., 2009; Lee et al., 2014; Lim et al., 2008; Tamis et al., 2014; Zhang et al., 2009). Pardelha et al. have proposed a model that extends the production of P(HB-co-HV) to a complex mixture of fatty acids. In this specific case, based on their number of carbons, VFA go through different pathways that convert them either to acetyl-CoA or propionyl-CoA (Pardelha et al., 2012). This principle has been generalized by Tamis et al. who have proposed a model describing the feast and famine process of PHA accumulating culture, fed with a mixed substrate. Each substrate is dedicated to hydroxubutyrate, hydroxyvalerate or biomass productions (Tamis et al., 2014). Recently, a model of PHA production process using a mixture of acetate, propionate, butyrate, and valerate has been developed, considering that all these carbon sources are not simultaneously assimilated but rather follow a sequential pattern. The proposed kinetic structure describes the phenomenon as an inhibition of one VFA by the other (Wang et al., 2018).

Some purple bacteria such as *Rs. rubrum* have demonstrated the ability to produce various polymers when growing on VFA (Bayon-Vicente et al., 2020b; Brandl et al., 1989; De Meur et al., 2020). Studies carried on purple non-sulfur bacteria (PNSB) have highlighted that when VFA are present in a mixture, their assimilations do not occur simultaneously, rather following a sequential pattern of assimilations, and that the presence of a co-substrate could have a synergic effect leading to an increase of VFA uptake rates (Alloul et al., 2022, 2019; Cabecas Segura et al., 2021; Fradinho et al., 2014). These models only describe the production of PHA during nitrogen limiting conditions and bacterial growth is therefore not considered. In *Rs. Rubrum*, PHA production occurs even when no nutrient is lacking in the culture medium but is rather driven by redox imbalance in the cell, and as such occurs during biomass production (Bayon-Vicente et al., 2020a; Cabecas Segura et al., 2022a, 2022b).

The aim of this study is to derive a mathematical model to predict qualitatively and quantitatively the PHA production and composition while considering the substrate competition during biomass production in a culture of *Rs. rubrum*, a model organism for purple bacteria.

## 2. Materials and methods

### 2.1. Bacterial strain and culture conditions of Rs. rubrum

The considered strain is Rhodospirillum rubrum S1H (ATCC15903). The growth basal medium used for photoheterotrophic culture conditions of *Rs. rubrum* is the basal salt medium of Segers and Verstraete (1983) described by Suhaimi et al. (1987), which was supplemented with $NH_4CI$ (35 mM) as the nitrogen source, $NaHCO_3$ (50 mM), and biotin (0.06 mM). Different mixtures of VFA were used as carbon sources with the same net carbon concentration of 124 mM of equivalent carbon. The pH was adjusted to 6.9. *Rs. rubrum* was grown under anaerobic phototrophic conditions in 50 ml sealed serum flasks under 50 μmole $m^{-2}\ s^{-1}$ of light intensity supplied by halogen lamps (Sencys; 10 W; 100 lumens; 2650 K), at 30 °C with a rotary shaking at 200 rpm. Each culture condition was achieved with five biological replicates, excepted the cultivation experiments. Nitrogen gas was used to purge oxygen from the upper gas phase and the flasks were hermetically sealed. The growth was monitored following the turbidity at $OD_{680\ nm}$, initially set between 0.4 and 0.5 after inoculation. A correlation curve between OD and biomass dry weight was used to convert $OD_{680\ nm}$ in biomass content.

### 2.2. Monitoring of VFA content

The monitoring of VFA concentration in the culture medium was performed on culture supernatants obtained by centrifugation at 16,000 *g* for 10 min at 4 °C and stored at − 20 °C before analysis. Aliquots (100 μl) of culture supernatant were analyzed by HPLC-refractometry (Waters 2695 separation Module; Waters 2414 Refractive Index Detector). The separation was done in isocratic mode using a Shodex Sugar SH1011 column (300 mm × 8 mm) with 5 mM $H_2SO_4$ as mobile phase. The detection was performed by refractometry at 210 nm. The amounts of acetate, propionate, butyrate, and succinate were determined by integrating their specific peaks and comparisons to standard curves ($R^2 >$ 0,99). The concentrations of VFA were therefore obtained by correlation with the corresponding peak underlying area (i.e., *[VFA]* = *a* * *[area]*, where "*a*" stands as linear coefficient of the correlation curve and *[VFA]* is the concentration in *mM*).

### 2.3. PHA monomer quantification

The PHA content determination was adapted from a method described in the literature (Snell et al., 2002). To determine the PHA composition and content, 500 μl of culture broth was centrifuged at 8000 rpm during 5 min. The pellet was resuspended with 500 μl of chloroform and added in a 10 ml screw cap glass tubes with 2 ml of a solution containing 1.94 ml of methanol, 0.06 ml of sulfuric acids, 0.2 mg of toluic acids. The tubes were then put in a thermostatically regulated bath at 100 °C for 210 min. This method degrades intracellular PHA by methanolysis to its constituent hydroxycarboxylic acid methyl esters. After the reaction, 1 ml of distilled water was added and the tube was shaken vigorously. After phase separation, the organic phase (bottom layer) was removed and transferred to a small screw cap glass vial. Those methyl esters were analyzed using gas chromatography with the help of a SHIMADZU GC-MS QP2010S equipped with an Optima ® 5 capillary column (30 m/0.25 nm; Macherey-Nagels) and a flame ionization detector. Further, 2 μl portion of the organic phase is analyzed after spitless injection. Helium (20.2 ml/min) was used as the carrier gas. The temperatures of the injector were 250 °C.

### 2.4. Model identification procedure

The proposed modeling approach is based on a priori knowledge of the metabolic network and data obtained from the in-lab experiments described hereafter in Section 3.1 (Fig. 1).

The considered bioprocess can be described by the following macroscopic reaction scheme:

$$\sum_{i\in\mathbb{R}_k} k_{i,k}\xi_i \xrightarrow{\varphi_k} \sum_{j\in\mathbb{P}_k} k_{j,k}\xi_j \tag{1}$$

with $k \in [1, M]$ where M is the number of reactions, $\mathbb{R}_k$ and $\mathbb{P}_k$ denote

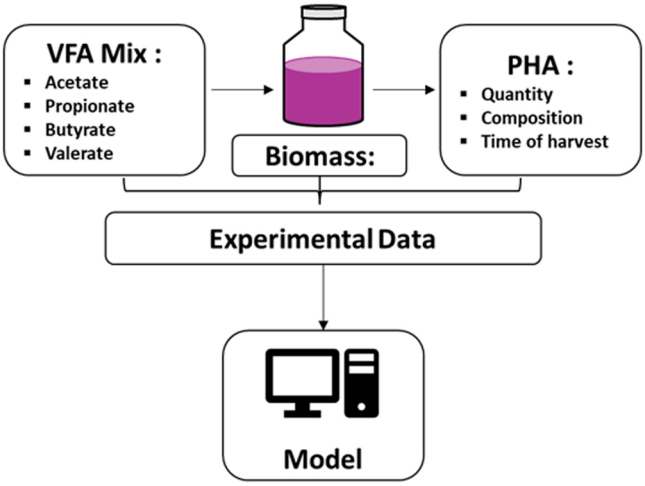


**Fig. 1.** Schematic diagram of the experimental setup.

respectively the set of reactants and products in the reaction k. The parameters $k_{i,k,}$ and $k_{j,k}$ are the pseudo stoichiometric coefficients while $\varphi_k$ is the corresponding reaction rate. Applying mass balance to (1), the following ordinary differential equation (ODE) system is obtained, describing the variations of each species concentration with time:

$$\frac{d\xi(t)}{dt} = K\varphi(\xi, \theta_\varphi, t) \tag{2}$$

where K is the pseudo-stoichiometric matrix and $\theta_\varphi$ the kinetic parameters. Parameter estimation is conducted by minimizing a least-squares criterion measuring the distance between model-simulated data $\xi_m$ and experimental measurements $\xi_{exp}$ as in:

$$J(\theta) = \left(\xi_m(\theta) - \xi_{exp(\theta)}\right)^T Q^{-1} \left((\xi)_m(\theta) - \xi_{exp(\theta)}\right) \tag{3}$$

where θ is the parameter vector (gathering stoichiometric and kinetic parameters).

The initial state $\xi_0$ is a vector of length N times nexp, the latter being the number of used experiments and N the size of vector ξ, that is, the number of studied macroscopic species (in the current case, biomass, VFAs and PHAs). $\xi_0$ represents the set of state variable initial conditions inferred from the experimental measurements at time t = 0. Q is the measurement error covariance matrix designed as a diagonal matrix with the squares of the maximum respective concentration levels to normalize the distances calculated in (3), which is of good practice when measurement error distributions are not a priori known. Parameter identification is performed with the MATLAB optimizer "fminsearch", achieving the Nelder-Mead algorithm which is efficient in preventing the optimization from ending in local minima.

The data sets obtained from three biological replicates are used for parameter estimation purpose and model direct validation. Local parameter identifiability and sensitivity analysis are addressed based on the Fisher Information Matrix (FIM), which can be computed as follows:

$$FIM = \sum_{tk=1}^{n_{meas}} \left(\xi_{\theta,i}(t_k, \widehat{\theta})\right)^T Q^{-1} \xi_{\theta,i}(t_k, \widehat{\theta}) \tag{4}$$

where $t_k$ is the sampling time and $n_{meas}$ is the number of samples. A lower (Cramer-Rao) bound of the parameter estimation error covariance matrix can be obtained as follows:

$$\widehat{P} > \sigma^2 FIM^{-1} \tag{5}$$

with $\sigma^2$ being the a posteriori estimate of the measurement error variance calculated from the residual cost function $J^*$ at the optimum:

$$\sigma^2 = \frac{J^*}{nexp * N_{meas} - n_\theta} \tag{6}$$

where $N_{meas}$ is the total number of measurements (nmeas times N) and $n_\theta$ is the number of estimated parameters.

## 3. Results

### 3.1. Typical process behavior

In a waste stream, VFAs are present in a mixture, whose composition varies according to fermentation parameters. Nonetheless, the most commonly found VFAs are acetate, propionate, butyrate, and valerate (Dahiya et al., 2015; Jiang et al., 2013; Komemoto et al., 2009; Lee et al., 2014; Zhang et al., 2009). The macroscopic phenomenon occurring during the assimilation of a mixture of those 4 VFAs by *Rs. rubrum* and the resulting polymer productions are presented in Fig. 2.

The assimilation of VFAs follows a sequential pattern. Indeed, as already described in the literature, the assimilation of butyrate is inhibited by the presence of acetate and/ or propionate in the medium (Paloma; Cabecas Segura et al., 2022a, 2022b). Interestingly, valerate consumption is also delayed in presence of acetate and propionate (Fig. 2). A two-step process can thus be observed: acetate and propionate are first assimilated simultaneously and then butyrate and valerate are concomitantly consumed. Conversely to numerous PHA production processes, where biomass production and PHA accumulation are decoupled, here, polymer accumulation occurred during biomass growth. In *Rs. rubrum* and the present operating conditions, PHA production is supposed to be used as a redox balance mechanism to help dealing with the redox stress engendered by the assimilation of substrate more reduced than biomass such as VFA and therefore occurring during biomass production (Bayon-Vicente et al., 2020a). The highest polymer concentration is observed at the end of the exponential phase, before complete assimilation of the available carbon source. When carbon becomes limiting, the global PHA content decreases (Fig. 2). As PHAs are traditionally used as internal carbon storage means, the decrease in PHA content can be due to the absence of an alternative carbon source at this point, leading the cells to use the carbon stored intracellularly in the form of PHAs.

When this mixture of VFAs is used as a carbon source, it can be observed that the produced polymer is actually a copolymer of HB and

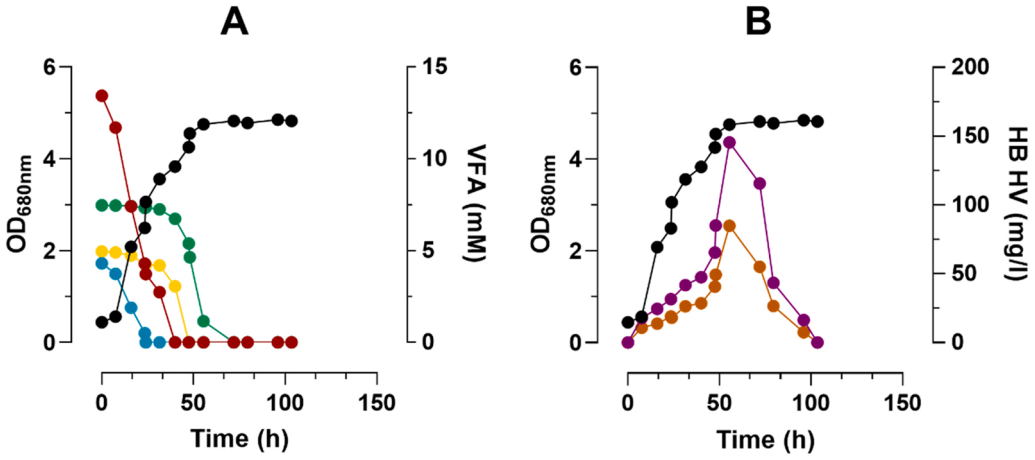


**Fig. 2.** Monitoring of biomass (●), HB (●) and HV (●) productions (B) during photoheterotrophic assimilations of acetate (●), propionate (●), butyrate (●), and valerate (●) by *Rs. rubrum* (A).

HV. This composition is consistent with the literature, which demonstrates that, during assimilation of acetate (Bayon-Vicente et al., 2020a) and butyrate (De Meur et al., 2020), *Rs. rubrum* produces PHB, while, in presence of propionate (Cabecas Segura et al., 2021) or valerate (Bayon-Vicente et al., 2020b), polymers with a high level of HV are obtained. The presence of HB and HV in the obtained polymer from a mixture of acetate, propionate, butyrate, and valerate, could therefore be expected. A schematic representation of substrate impact on the polymer composition is presented in Fig. 3.

A mathematical model describing the substrate uptake and polymer production of the 15 possible combinations of carbon sources containing 1,2,3 or 4 VFAs among the most produced during waste stream fermentation (acetate, propionate, butyrate, and valerate) were developed. The different case scenarios and their particularities in terms of substrate competition and polymer composition are presented in Table 1. The production of polymer from propionate being extremely low (less than 2 % of the biomass), this case will not be presented in this study.

### 3.2. Description of substrate preference

Macroscopic dynamic models with a good predictive capability have been proposed for the growth of *Rs. rubrum* using every VFA mixture containing acetate, propionate, and/or butyrate, to provide an accurate prediction of the occurring substrate competition (Cabecas Segura et al., 2022a, 2022b). Different kinetic models were proposed but the best prediction was obtained when an inhibition factor was added to the butyrate uptake rate. In this work, it will be assumed that the observed "delay" in valerate assimilation in presence of acetate and/or propionate can be similarly described.

### 3.3. Description of the production and consumption of PHA general structures

As the proteomic analysis tends to indicate simultaneous production and consumption of PHA along with the bacterial growth, the consumption of PHA is assumed to be likely to occur from the start of the culture rather than punctually, following a switch phenomenon (Bayon-Vicente et al., 2020b; Cabecas Segura et al., 2021; De Meur et al., 2020). Therefore, simple Monod kinetics, combined with inhibition factors, shown in Table S1 of the Supplementary material, are proposed as potential model candidates. For a specific substrate $S$ and biomass $X$, Monod kinetics read:

$$\varphi = X \quad \mu_{max} \frac{S}{K_S + S} \tag{7}$$

where $\mu_{max}$ is the maximal uptake rate coefficient (in $h^{-1}$), $S$ and $X$ are respectively the substrate and biomass concentrations (in g/l) and $K_S$ is the half-saturation constant (g/l). The latter characterizes the substrate concentration level at which the rate reaches half of its maximum value,

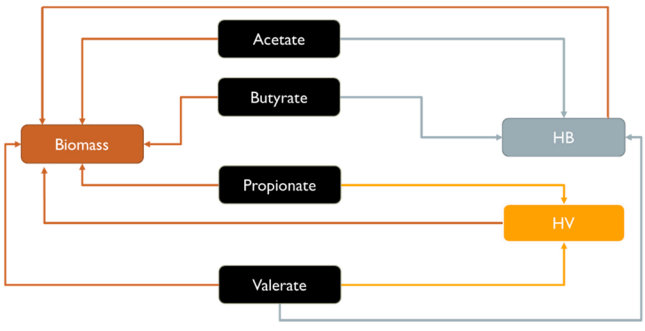


**Fig. 3.** Schematic representation of polymer production by *Rhodospirillum rubrum*.

inducing activation effect at low substrate concentration levels and saturation at high ones. Expression (7) can also be complemented with inhibition factors assuming that the presence of some other metabolites may decrease the corresponding rate. In this particular case, Eq. (7) becomes:

$$\varphi = X \quad \mu_{max} \frac{S_1}{K_S + S_1} \frac{K_{iS2}}{K_{iS2} + S_2} \tag{8}$$

where $K_{iS2}$ (g/l) stands as inhibition constant. Eq. (8) describes a rate that is activated by a substrate $S_1$ while being inhibited by a second substrate $S_2$. It can be noticed that when $S_2 = K_{iS2}$, the inhibition factor divides the rate by two.

Based on the monitoring of PHA production in cultures of *Rs. rubrum*, PHA consumption is assumed to be related to biomass growth. As shown by the cost function residual presented in Table 2, model biomass predictions are relatively poor. Regarding parameter estimation accuracy, the tightness of the confidence intervals shows that almost all parameters are locally identifiable. However, the stoichiometric coefficients (written $C_i$ in the following tables and Supplementary material, and indicating a substrate to biomass yield for component i (in g/g); $hb_{pi}$, $hv_{pi}$ are therefore respectively substrate to hydroxybutyrate and hydroxyvalerate monomer yield coefficients of component i (g/g) and $hb_c$, $hv_c$ respectively hydroxybutyrate and hydroxyvalerate monomer to biomass yield coefficients of component i (g/g)) present orders of magnitude which are not in accordance with the previously obtained values and the saturation constants have wide confidence intervals, suggesting an over-parametrization of the system (Table 2). To improve the biomass fitting, cell death rate (μd ($h^{-1}$)) has been considered but unfortunately without success as shown in Table 2.

Since the polymer consumption starts with the biomass stationary phase, another possibility would be to involve PHA consumption in the biomass maintenance mechanism. The residual of the corresponding optimization seems to be of equivalent order of magnitude whatever the conditions (Table 2). All parameters are locally identifiable excepted the stoichiometric coefficient and the growth rate involved in the PHA consumption. One last possibility that should be considered is that the consumption of PHA is assumed to be inhibited by the presence of carbon sources in the medium. Therefore, the addition of an inhibition factor in the PHA consumption rate expression could help to improve the fitting. The residual related to this last proposition is much lower than in the previous cases, indicating it as the best structural assumption.

### 3.4. Model reduction for the different case scenarios

Based on the observation of the process behavior and the knowledge gathered on *Rs. rubrum* production of PHAs from VFAs, the following assumptions were made and applied to all case scenarios: (i) Acetate and propionate inhibit butyrate and valerate assimilations, (ii) Acetate and Butyrate only produce HB, while (iii) propionate leads to the production of only HV and (iv) valerate to both HB and HV. (v) Polymers are concurrently produced and consumed but their consumption is inhibited by the presence of carbon substrate in the culture medium. The development of the mathematical model describing PHA production when acetate and butyrate are used as carbon sources will be considered as a validating and didactic example of the above-mentioned assumptions. The different kinetic structure and mass balances are presented in Table S2.

As confirmed by the residual of the cost function, the fitting between model predictions and experimental data is satisfactory (Table 3). However, regarding parameter estimation, local identifiability is verified excepted for the different uptake rates and the stoichiometric coefficient describing the conversion of acetate in HB, which exhibits high confidence of interval (Table 3). During the development of models describing the assimilations of VFAs in *Rs. Rubrum* (Paloma; Cabecas Segura et al., 2022a, 2022b), considering the same assimilation rate for

**Table 1**
Different case scenarios describing PHA production by *Rs. rubrum* growing on different mixtures of acetate, propionate, butyrate, and valerate.

| Polymer | | PHB | | | P (HB-*co*-HV) | | | | | | | | | | |
|---|---|---|---|---|---|---|---|---|---|---|---|---|---|---|---|
| Inhibition | | – | – | $S_3$ by $S_1$ | – | – | – | $S_3$ by $S_2$ | $S_4$ by $S_1$ | $S_4$ by $S_2$ | $S_3$ & $S_4$ by $S_1$ | $S_3$ & $S_4$ by $S_2$ | $S_3$ by $S_1$ by $S_2$ | $S_4$ by $S_1$ by $S_2$ | $S_3$, & $S_{4'}$ by $S_1$ & $S_2$ |
| Acetate | $\mathbf{S_1}$ | X | | X | | X | | | X | | X | | X | X | X |
| Propionate | $\mathbf{S_2}$ | | X | | | X | | X | | X | | X | X | X | X |
| Butyrate | $\mathbf{S_3}$ | | | X | | | X | X | | | X | X | X | | X |
| Valerate | $\mathbf{S_4}$ | | | | X | | X | | X | X | X | X | | X | X |
| Case | | $A_1$ | $A_2$ | B | C | $D_1$ | $D_2$ | $E_1$ | $E_2$ | F | G | H | I | J | K |

**Table 2**
Parameter estimation of the model describing polymer (PHB) production and consumption during photoheterotrophic assimilations of acetate (ace) and butyrate (but) by *Rs. rubrum. Several hypotheses regarding polymer consumption are considered: (1) Monod kinetics without reconsumption, reconsumption during cell death described by a (2) constant or a (3) variable rate, (4) consumption for cellular maintenance or (5) reconsumption for biomass growth when VFA are no longer available. The resulting parameter estimations are provided with the corresponding confidence intervals (CI %).*

| | Biomass production (1) | | Constant cell death rate (2) | | Variable cell death rate (3) | | Cellular maintenance (4) | | PHA consumption inhibited by substrate (5) | |
|---|---|---|---|---|---|---|---|---|---|---|
| | Value | CI (%) | Value | CI (%) | Value | CI (%) | Value | CI (%) | Value | CI (%) |
| $\mu max_{ace}$ | 0.043 | 1.78E + 03 | 1.51E + 04 | 1.00E + 02 | 0.051 | 1.02E + 03 | 0.139 | 980.484 | 0.1292 | 3.30E + 02 |
| $\mu max_{but}$ | 0.004 | 9.37E + 04 | 0.025 | 9.62E + 03 | 0.005 | 2.55E + 04 | 0.105 | 490.562 | 0.0593 | 7.20E + 02 |
| $\mu max_{hb}$ | 0.001 | 5.92E + 05 | 0.008 | 3.03E + 04 | 0.020 | 1.42E + 04 | 0.115 | 1.18E + 08 | 0.0259 | 1.65E + 02 |
| $k_{ace}$ | 1.005 | 8.40E + 02 | 1.002 | 2.37E + 02 | 1.014 | 3.13E + 02 | 1.007 | 241.373 | 1.0000 | 4.29E + 00 |
| $k_{but}$ | 1.021 | 2.59E + 03 | 1.003 | 2.29E + 01 | 0.988 | 4.02E + 02 | 0.993 | 610.544 | 0.5942 | 7.21E + 00 |
| $k_{hb}$ | 0.975 | 5.76E + 03 | 0.999 | 2.23E + 04 | 1.004 | 3.03E + 04 | 0.995 | 1211.775 | 1.1003 | 3.89E + 00 |
| $ki_{ace}$ | 1.001 | 9.71E + 02 | 0.995 | 1.60E + 02 | 1.013 | 1.24E + 02 | 0.996 | 316.546 | 1.0007 | 4.28E + 00 |
| $C_{ace}$ | 47.239 | 7.72E + 01 | 1.10E + 04 | 6.71E + 05 | 11.364 | 9.47E + 02 | 0.849 | 57.081 | 0.3768 | 1.14E + 01 |
| $C_{but}$ | 48.345 | 9.19E + 01 | 3.723 | 9.71E + 03 | 29.700 | 2.55E + 04 | 0.348 | 55.138 | 0.8087 | 5.30E + 00 |
| $hb_{pa}$ | 4.040 | 8.67E + 01 | 0.010 | 2.03E + 07 | 1.924 | 9.63E + 02 | 0.000 | 9.71E + 03 | 0.4232 | 1.01E + 01 |
| $hb_{pb}$ | 33.449 | 8.83E + 01 | 19.503 | 9.61E + 03 | 0.649 | 2.70E + 04 | 0.401 | 130.434 | 0.0011 | 4.02E + 03 |
| $hb_c$ | 0.146 | 7.34E + 01 | 0.753 | 3.55E + 02 | 0.039 | 8.18E + 01 | 0.460 | 1.18E + 08 | 0.3326 | 1.29E + 01 |
| $ki_s$ | – | – | – | | – | | – | – | 2.5791 | 1.66E + 00 |
| $\mu d$ | – | – | 0.005 | 1.03E + 09 | 0.053 | 1.71E + 02 | – | – | 0.2354 | |
| $ki_d$ | – | – | – | – | 0.998 | 2.40E + 02 | – | – | – | – |
| J | 1.682 | – | 1.710 | – | 1.647 | – | 0.335 | – | 0.335 | – |

**Table 3**
Parameter estimation results following model reductions, describing polymer (hb) production during photoheterotrophic assimilations of acetate (ace) and butyrate (but) by *Rs. rubrum. Each parameter value is provided with the corresponding confidence interval (CI %). Several model reductions are considered, (1) applying the same uptake rate for all VFA present in the medium, (2) to both PHA and VFA, considering the production of PHA by only (3) acetate or (4) butyrate, and (5) applying the same stoichiometric coefficient for PHA production from all carbon sources.*

| | | | Common rate for VFA (1) | | Common rate for VFA and PHA (2) | | PHA produced only by acetate (3) | | PHA produced only by butyrate (4) | | Stoichiometric coefficient reduction (5) | |
|---|---|---|---|---|---|---|---|---|---|---|---|---|
| | Value | CI (%) | Value | CI (%) | Value | CI (%) | Value | CI (%) | Value | CI (%) | Value | CI (%) |
| $\mu max_{ace}$ | 0,13 | 330,18 | – | – | – | – | – | – | – | – | – | – |
| $\mu max_{but}$ | 0,06 | 720,28 | – | – | – | – | – | – | – | – | – | – |
| $\mu max_{hb}$ | 0,03 | 165,32 | 0,06 | 370,05 | – | – | – | – | – | – | – | – |
| $\mu max_{VFA}$ | – | – | 0,09 | 115,64 | – | – | – | – | – | – | – | – |
| $\mu max$ | – | – | 0,08 | 130,05 | 0,08 | 161,69 | 0,08 | 156,42 | 0,08 | 150,42 | 0,11 | 75,89 |
| $k_{ace}$ | 1,00 | 4,29 | 0,50 | 20,83 | 0,99 | 13,72 | 0,11 | 175,89 | 0,33 | 34,83 | 0,90 | 9,09 |
| $k_{but}$ | 0,59 | 7,21 | 1,02 | 10,26 | 1,00 | 13,64 | 0,90 | 9,09 | 1,19 | 9,58 | 1,23 | 6,66 |
| $k_{hb}$ | 1,10 | 3,89 | 0,96 | 10,88 | 1,00 | 13,61 | 1,23 | 6,66 | 0,57 | 19,96 | 5,75 | 1,43 |
| $ki_{ace}$ | 1,00 | 4,28 | 0,40 | 26,38 | 0,97 | 14,05 | 5,75 | 1,43 | 0,31 | 37,05 | 0,38 | 21,40 |
| $ki_{hb}$ | 0,38 | 11,37 | 0,03 | 409,54 | 0,89 | 15,30 | 0,38 | 21,40 | 0,04 | 302,00 | 1,27 | 6,47 |
| $c_{ace}$ | 0,81 | 5,30 | 0,66 | 15,95 | 1,17 | 11,62 | 1,27 | 6,47 | 0,61 | 18,76 | 0,80 | 10,25 |
| $c_{but}$ | 0,42 | 10,13 | 0,53 | 19,85 | 0,49 | 27,95 | 0,80 | 10,25 | 0,75 | 15,10 | 0,46 | 17,65 |
| $hb_{pa}$ | 0,00 | 4,02E + 03 | 0,12 | 3,36E + 05 | 0,00 | 1,16E + 05 | – | – | 0,11 | 103,66 | – | – |
| $hb_{pb}$ | 0,33 | 12,89 | 0,87 | 12,01 | 0,38 | 35,87 | 0,46 | 17,65 | – | – | – | – |
| $hb_p$ | – | – | – | – | – | – | – | – | – | – | 0,50 | 16,47 |
| $hb_c$ | 2,58 | 1,66 | 0,25 | 4,71 | 0,61 | 22,38 | 0,50 | 16,47 | 0,47 | 24,22 | 2,93 | 2,80 |
| J | 0,33 | | 0,34 | | 0,32 | | 0,33 | | 0,33 | | 0,23 | |

every VFA significantly improved the identifiability of the parameters. In the case of acetate and butyrate, when the same uptake rate is applied, the accuracy of the parameter estimation is, without real surprise, also improved (Table 3). Nonetheless, a high confidence interval is still observed for the uptake rate of HB. Comparably to what was assumed for VFA assimilation rates, the same maximum uptake rate to HB and HV was applied. The obtained results consolidate this observation via a better fitting of model predictions with the experimental data.

The stoichiometric coefficient related to HB production from acetate is the only parameter that remains poorly identifiable. When the model is reduced and does not take into consideration the conversion of acetate in HB, the residual cost function is low and all parameter estimations present small confidence intervals. Interestingly, when the production of HB from butyrate is removed from the model, similar results are

obtained. This tends to indicate that the model does not dissociate the production of HB coming from the conversion of acetate, from the HB produced during butyrate assimilation. From a biological point of view, it is not likely that HB production comes from only one of the carbon sources. In addition, the production of HB from both substrates occurs via the uptake of (R)-hydroxybutyrate by the polymerase.

It is thus proposed to gather acetate and butyrate conversions in hydroxybutyrate under the same stoichiometric coefficient. This model anew exhibits the lowest cost function residual and the best parameter estimation accuracy among all tested assumptions.

The application of a common rate for all VFA and PHA consumptions and a single common average stoichiometric coefficient describing the synthesis of one type of monomer from all VFAs allow to obtain a compact model with good preciseness and acceptable parameter estimation accuracy for 15 mixture conditions out of the 16 developed models. Only the model describing the assimilation of 4 VFAs (case K)

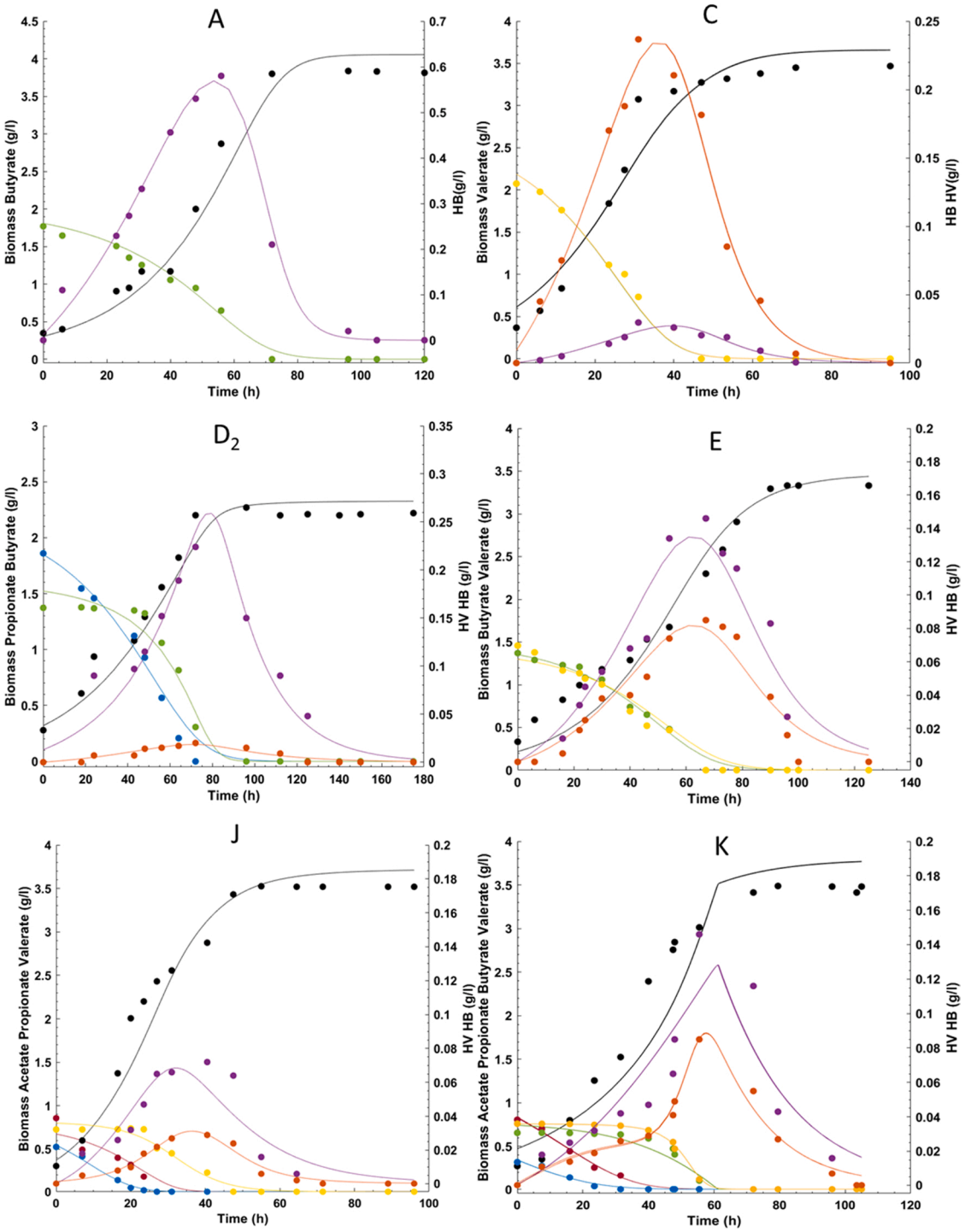


**Fig. 4.** Monitoring of biomass (●), HB (●) and HV (●) productions during photoheterotrophic assimilations of acetate (●), propionate (●), butyrate (●) and/or valerate (●) by *Rs. Rubrum*. For the sake of clarity, confidence intervals have been removed but the corresponding standard deviations are provided in Table S5 in the Supplementary material.

still exhibits some high parameter uncertainty. In this case, the inhibition constant describing the propionate effect on butyrate and valerate is not identifiable. Only one inhibition constant for both acetate and propionate is therefore proposed and tested. This allowed to significantly reduce the cost function residual and to return to acceptable parameter estimation accuracy. The final kinetic structure and mass balances are presented in Tables S3 and S4 respectively.

## 4. Discussion

In Fig. 4, the measured data and the respective predictions of the calibrated models describing each scenario are presented.

### 4.1. Model structure

The models can accurately describe the macroscopic phenomena occurring during the photoheterotrophic assimilation of *Rs. rubrum* growing on a different mixtures of carbon sources containing from 1 to 4 VFAs. The presence of an inhibition factor allows the description of the preferential selection of acetate and/or propionate on butyrate and/or valerate during VFA assimilation.

A minor deviation was however observed for culture growing on propionate and butyrate or propionate, butyrate and valerate (Cases D2 and H). In binary conditions, the inhibition ($K_i$) constant is relatively low ranging, indicating a phenomenon which is close to a switch from one carbon source to the other only when the first one has almost completely vanished. We therefore suggest that the inhibition of acetate on butyrate could be due to the fact that acetate inhibits the enzyme responsible of the inlet of butyrate in the central metabolism.

### 4.2. Parameter estimation

The parameters involved in the production and the consumption of the least produced monomers are the least accurately estimated (Table 4). This may be due to the fact that the data from the related polymer productions present higher relative measurement noise levels. This might either be due to the biological variability which is important regarding the quantity of produced PHAs, regardless of the conditions, or the concentration orders of magnitude of these specific monomers which are close to the detection sensitivity of the analytical instrument. In addition, the poor identifiability of parameters describing polymer consumption could be due to the limited number of data samples obtained during this process phase. The imprecision on those parameters may have repercussions on the accuracy of the maximum growth rate estimation. As a consequence, biomass growth, even if still satisfactory, exhibits the most important deviation in all cases.

Interestingly, the addition of an inhibition factor in the PHA consumption kinetic structure is also required to provide accurate descriptions of PHA accumulations in the biomass. This kinetic structure leads to an accurate prediction of PHA production peak which is a crucial point in the development of the corresponding biotechnological PHA production process. Indeed, regardless of the case scenario 10 H, more than half of the polymer is consumed. In addition to the amount of produced polymer, once starting to be assimilated, the length of the polymer chain, which defines the mechanical and thermal properties of the material, may change and therefore becomes critical. One last aspect that must be taken into consideration is that in the case of sequential assimilation of the substrate, if complete assimilation is not observed, the composition of the polymer and as such once again the properties of the polymer, may be impacted.

### 4.3. Impact of carbon source on PHA production

Traditionally, PHAs are accumulated as carbon storage polymers, when a nutrient such as nitrogen or phosphorus is depleted in the environment of the cell. The carbon/nitrogen or carbon/phosphorus ratio in the medium used in this work, is lower than in the biomass, indicating that bacterial growth is limited first by the carbon availability (Cabecas Segura et al., 2021). In this condition, PHA production seems to be triggered by something else than nutrient starvation.

PHA synthesis is often recognized as a redox balancing mechanism, and several conditions known to disrupt the redox homeostasis of *Rs. rubrum* cell, such as bicarbonate limitation or increase of light intensity, resulting in an increase of polymer production (Bayon-Vicente et al., 2020b, 2020a; Cabecas Segura et al., 2021). Likewise, culture presenting substrate adaptation or growing in bicarbonate excess condition, phenomena known to help the cells to deal with redox imbalance, tending to exhibit lower PHA accumulation.

The low production of PHA observed when several carbon sources are used simultaneously (around 12 % of the biomass weight) may therefore arise from a better ability of the cells to deal with redox imbalance (Cabecas Segura et al., 2021). In addition, data recently reported and supported by previous studies, indicate that *Rs. rubrum* could use the isoleucine biosynthesis pathway to help maintaining redox homeostasis during photoheterotrophic metabolism (Bayon-Vicente et al., 2021, 2020b, 2020a; De Meur et al., 2020; McCully et al., 2019). In mixture conditions, this pathway and the synthesis of $H_2$ may be used for redox homeostasis relaxing the requirement of PHA production (Cabecas Segura et al., 2021).

When only one VFA is used as a carbon source, the reduced state of the substrate was not linked to a higher PHA accumulation in the biomass. Indeed, acetate and butyrate leads to the highest PHA content. This may be due to the fact that from acetyl-CoA only, the synthesis of HB consumes a redox equivalent. In addition, the synthesis of PHA is only essential for *Rs. rubrum* growth to occur when acetate is the carbon source (De Meur and Wattier, 2017). Another possibility would be that acetate is assimilated via the EMC pathway, that shares some common intermediates with PHA synthesis (Cabecas Segura et al., 2021; De Meur et al., 2020). In this context, the flux through the EMC pathway and thus through the first enzymes of the PHA biosynthesis, promotes PHA accumulation. The production of HB and HV competes with acetyl-CoA and propionyl-CoA utilizations for other biosynthesis pathways and may explain why when propionate or valerate is used as carbon source, the production of PHA is lower than in the case of acetate or butyrate, where acetyl-CoA is more readily available. The higher content of PHA, observed in the butyrate condition, is more difficult to explain. Even if crotonyl CoA is a key intermediate in butyrate assimilation, the enzymes involved in its conversion in (R) hydroxybutyryl-CoA, the primary intermediate of PHA production, are not up-regulated. In *Rs. rubrum,* it was hypothesized that the presence of polymerase was sufficient to induce PHA production, as all the reactions occurring before can be catalyzed by different enzymes. For an unknown reason, the PHA polymerase is strongly upregulated by the presence of butyrate (Hustede et al., 1993).

Nonetheless, the yield of HB and HV productions from VFA, obtained during parameter estimation of the different models, were higher in cultures containing butyrate, while the presence of propionate in the initial carbon mixture seemed to have a deleterious effect on PHA production. This phenomenon was also observed during other PHA accumulation processes, i.e. in *Rb. sphaeroides,* where acetate and butyrate lead to a higher rate of PHA production. Conversely, the presence of propionate in the culture medium tends to decrease the PHA content of the cell (Fradinho et al., 2014). This was also observed at the enzymatic level when proteomic analyses where carried out on a mixture of propionate and butyrate. The data showed that PHA synthase (Rru_A2413) was highly upregulated when butyrate was used as a carbon source in comparison with propionate only (Cabecas Segura et al., 2021). However, in the mixture condition during the propionate assimilation phase, this enzyme was upregulated in comparison with the propionate-only condition. *In Rs. rubrum*, it was demonstrated that the polymerase was the only necessary enzyme to maintain polymer production (Hustede et al., 1993). It can therefore be hypothesized that the presence of

**Table 4**
Parameter estimation results following model reductions, describing polymer (hb, hv) productions during photoheterotrophic assimilations by *Rs. rubrum* of the 15 different mixtures of VFAs. These models describe VFA sequential assimilation and VFA preferential assimilation (considering inhibition effects) using the same maximal uptake rate constant. Each parameter value is provided with the corresponding confidence interval (CI %).

*A: Model describing the production of PHA by Rs. rubrum when one VFA is used as carbon source.*
*Case A1; A2: acetate as carbon source; case C: valerate as carbon source.*

| | Case $A_1$ | | Case $A_2$ | | Case C | |
|---|---|---|---|---|---|---|
| | Value | Ci (%) | Value | Ci (%) | Value | Ci (%) |
| $\mu max_s$ | 0,049 | 417,78 | 0,056 | 374,44 | 0,074 | 487,11 |
| $K_{ace}$ | 0,988 | 20,55 | – | – | – | – |
| $K_{but}$ | – | – | 0,999 | 20,93 | – | – |
| $K_{val}$ | – | – | | | 1,015 | 35,70 |
| $K_{hb}$ | 1,000 | 20,30 | 1,024 | 20,43 | 0,999 | 36,25 |
| $K_{hv}$ | – | – | | | 1,447 | 25,03 |
| $Ki_{hb}$ | 0,998 | 20,34 | 1,000 | 20,92 | 0,924 | 39,19 |
| $K_{ihv}$ | – | – | – | – | 0,061 | 598,36 |
| $C_{ace}$ | 1,495 | 13,58 | – | – | – | – |
| $C_{but}$ | – | – | 0,744 | 28,10 | – | – |
| $C_{val}$ | – | – | – | – | 0,210 | 172,35 |
| $P_{hb}$ | 0,699 | 29,05 | 0,652 | 32,09 | 0,910 | 39,79 |
| $P_{hv}$ | – | – | – | – | 0,014 | 2601,34 |
| $C_{hbc}$ | 3,215 | 6,32 | 1,199 | 17,45 | 0,137 | 264,21 |
| $C_{hvc}$ | – | – | – | – | 0,362 | 99,98 |
| **Residu** | 0,05 | | 0,06 | | 0,41 | |

*B: Model describing the production of PHA by Rs. rubrum when a binary mixture of VFAs is used as carbon source*
*Case B; mix acetate/butyrate; Case D: mix acetate/propionate; Case E: mix acetate/valerate; Case F: mix butyrate/valerate*

| | Case $D_1$ | | Case B | | Case $E_2$ | | Case $E_1$ | | Case F | | Case $D_2$ | |
|---|---|---|---|---|---|---|---|---|---|---|---|---|
| | Value | Ci (%) | Value | Ci (%) | Value | Ci (%) | Value | Ci (%) | Value | Ci (%) | Value | Ci (%) |
| $\mu max_s$ | 0,091 | 37,39 | 0,108 | 75,89 | 0,103 | 626,65 | 0,031 | 204,36 | 0,041 | 242,50 | 0,018 | 555,70 |
| $K_{ace}$ | 0,916 | 3,73 | 0,902 | 9,09 | 0,997 | 64,75 | – | – | – | – | – | – |
| $K_{prop}$ | 0,871 | 3,92 | – | – | – | – | 0,544 | | 0,977 | 10,24 | – | – |
| $K_{but}$ | – | – | 1,231 | 6,66 | – | – | 0,648 | 45,78 | – | – | 1,099 | 20,97 |
| $K_{val}$ | – | – | – | – | 0,986 | 65,49 | – | 38,42 | 0,016 | 64,74 | 1,032 | 22,25 |
| $K_{hb}$ | 2,385 | 1,43 | 5,748 | 1,43 | 0,987 | 65,41 | 21,006 | 1,19 | – | – | 3,076 | 24,20 |
| $K_{hv}$ | 1,018 | 3,35 | – | – | 0,459 | 140,88 | 1,130 | 22,08 | 3,675 | 2,72 | 0,922 | 21,90 |
| $Ki_{ace\ on\ but}$ | – | – | 0383 | 21,40 | – | – | – | – | – | – | – | – |
| $Ki_{ace\ on\ val}$ | – | – | – | – | 0,123 | 55,20 | – | – | – | – | – | – |
| $Ki_{prop\ on\ but}$ | – | – | – | – | – | – | 0,350 | 71,07 | – | – | – | – |
| $Ki_{prop\ on\ val}$ | – | – | – | – | – | – | – | – | 0,152 | 65,81 | | |
| $Ki_{hb}$ | 0,222 | 15,40 | 1,267 | 6,47 | 1,029 | 62,75 | 0,184 | 135,54 | – | – | 0,078 | 21,33 |
| $Ki_{hv}$ | 1,104 | 3,09 | | | 1,099 | 58,76 | 1,017 | 24,45 | 0,999 | 10,02 | 1,518 | 21,16 |
| $C_{ace}$ | 0,564 | 6,05 | 0,800 | 10,25 | 1,125 | 57,37 | – | – | – | – | – | – |
| $C_{prop}$ | 1,000 | 3,41 | – | – | – | – | 1,401 | 17,77 | 1,151 | 8,69 | – | – |
| $C_{but}$ | – | – | 0,465 | 17,65 | 0,800 | 80,75 | – | 10,10 | – | – | 2,713 | 17,10 |
| $C_{val}$ | – | – | – | – | – | – | 2,463 | – | 0,578 | 17,31 | 0,145 | 20,69 |
| $P_{hbp}$ | 0,062 | 55,24 | 0,498 | 16,47 | 0,132 | 48,58 | 0,754 | 32,97 | – | – | 4,619 | 204,69 |
| $P_{hbv}$ | 0,022 | 157,91 | – | – | 0,075 | 161,53 | 0,017 | 142,68 | 0,083 | 120,56 | 0,418 | 169,68 |
| $C_{hbv}$ | 2,595 | 1,31 | 2,932 | 2,80 | 0,403 | 160,25 | 14,469 | 1,72 | – | – | 1,877 | 49,08 |
| $C_{hv}$ | 0,536 | 6,36 | – | – | 0,277 | 233,16 | 3,070 | 8,11 | 2,042 | 4,90 | 1,544 | 42,24 |
| **J** | 0,28 | | 0,23 | | 0,43 | | 0,55 | | 0,42 | | 0,35 | |

*C: Model describing the production of PHA by Rs. rubrum when a ternary and quaternary mixture of VFAs is used as carbon source Case G: mixture acetate/propionate/butyrate; case H: mixture acetate/propionate/valerate; case I: mixture acetate/butyrate/valerate; case K:acetate/ propionate/butyrate/valerate*

| | Case G | | Case H | | Case I | | Case J | | Case K | |
|---|---|---|---|---|---|---|---|---|---|---|
| | Value | Ci (%) | Value | Ci (%) | Value | Ci (%) | Value | Ci (%) | Value | Ci (%) |
| $\mu max_s$ | 0,037 | 757,11 | 0,03 | 158,71 | 0,03 | 343,09 | 0,06 | 355,25 | 0,035 | 1365,990 |
| $K_{ace}$ | 1,024 | 27,04 | 0,04 | 147,71 | 0,97 | 10,15 | – | – | 1,000 | 47,908 |
| $K_{prop}$ | 0,998 | 27,74 | 0,08 | 67,86 | – | – | 0,51 | 39,23 | 1,000 | 47,900 |
| $K_{but}$ | 0,849 | 32,50 | – | – | 0,09 | 108,29 | 1,00 | 20,06 | 1,005 | 47,661 |
| $K_{val}$ | – | – | 0,20 | 27,45 | 1,56 | 6,28 | 0,86 | 23,40 | 1,002 | 47,834 |
| $K_{hb}$ | 1,712 | 16,33 | 1,00 | 5,48 | 1,00 | 9,80 | 6,39 | 3,13 | 1,003 | 47,767 |
| $K_{hv}$ | 1,000 | 27,67 | 0,91 | 6,05 | 1,18 | 8,32 | 1,02 | 19,65 | 0,999 | 47,964 |
| $Ki_{ace\ on\ but}$ | 1,004 | 27,58 | – | – | 0,99 | 9,91 | – | – | – | – |
| $Ki_{ace\ on\ val}$ | 0,280 | 96,85 | 1,00 | 5,50 | 0,05 | 194,73 | – | – | – | – |
| $Ki_{prop\ on\ but}$ | 1,001 | 11,84 | – | – | – | – | 1,01 | 19,88 | – | – |
| $Ki_{prop\ on\ val}$ | 0,701 | 16,91 | 0,05 | 101,63 | – | – | 0,03 | 582,80 | – | – |
| $Ki_{on\ but}$ | – | – | – | – | – | – | – | – | 0,999 | 47,942 |
| $Ki_{on\ val}$ | – | – | – | – | – | – | – | – | 1,012 | 47,329 |
| $Ki_{hb}$ | 0,305 | 88,93 | 0,04 | 125,56 | 0,98 | 9,00 | 0,06 | 20,20 | – | – |
| $Ki_{hv}$ | 0,798 | 34,49 | 0,01 | 431,40 | 1,09 | 10,01 | 0,99 | 337,55 | 0,999 | 47,958 |
| $C_{ace}$ | 1,336 | 20,64 | 0,77 | 7,12 | 4,08 | 2,41 | 0,79 | 25,46 | 2,405 | 19,941 |
| $C_{prop}$ | 1,471 | 18,76 | 1,00 | 5,45 | | | 0,53 | 37,56 | 3,449 | 13,893 |
| $C_{but}$ | 0,772 | 35,67 | – | – | 0,45 | 21,82 | | | 0,768 | 62,391 |

(*continued on next page*)

**Table 4** (*continued*)

*C: Model describing the production of PHA by Rs. rubrum when a ternary and quaternary mixture of VFAs is used as carbon source Case G: mixture acetate/propionate/butyrate; case H: mixture acetate/propionate/valerate; case I: mixture acetate/butyrate/valerate; case K:acetate/ propionate/butyrate/valerate*

| | Case G | | Case H | | Case I | | Case J | | Case K | |
|---|---|---|---|---|---|---|---|---|---|---|
| | Value | Ci (%) | Value | Ci (%) | Value | Ci (%) | Value | Ci (%) | Value | Ci (%) |
| $C_{val}$ | – | – | 0,49 | 11,14 | 2,56 | 3,83 | 0,97 | 20,70 | 0,799 | 59,959 |
| $P_{hbp}$ | 0,325 | 84,86 | 0,03 | 169,28 | 0,12 | 83,26 | 0,07 | 278,03 | 0,144 | 333,695 |
| $P_{hbv}$ | 0,038 | 725,77 | 0,02 | 220,63 | 0,28 | 34,74 | 0,04 | 550,69 | 0,103 | 467,294 |
| $C_{hbv}$ | 1,121 | 24,74 | 3,45 | 1,59 | 0,45 | 21,95 | 2,45 | 8,16 | 0,400 | 119,903 |
| $C_{hv}$ | 0,159 | 172,11 | 2,00 | 2,74 | 0,69 | 14,32 | 0,17 | 115,84 | 0,545 | 87,915 |
| **J** | 1.35 | | 1,25 | | 1.45 | | 1.35 | | 2,15 | |

butyrate could be sufficient to increase polymerase abundance and as such the quantity of produced polymer in those conditions.

Another possibility to explain the disparity of polymer production from the different mixtures of VFA would be the rate of VFA assimilation. Proteomic analyses carried out during the studies of the different VFA assimilations highlighted the concomitant presences of enzymes involved in PHA synthesis and degradation (Bayon-Vicente et al., 2020b; Cabecas Segura et al., 2021; De Meur et al., 2020; Leroy et al., 2015). This phenomenon was also observed in other strains such as *Ralstonia eutropha* (Lawrence et al., 2005; Narancic et al., 2016; Taidi et al., 1995). In this case, if the consumption rate of PHA is constant, the maximum amount of PHA that can be produced by the cell is limited by the PHA production rate. Indeed, when the PHA production rate equals the PHA degradation rate, the maximum PHA content is reached. As propionate uptake rate is significantly lower than acetate or butyrate, the production rate of PHA from propionate is lower than in the case of butyrate and as such PHA synthesis equals PHA degradation at a lower PHA content when propionate is used as substrate.

The regulation of PHA consumption may also be discussed as it may influence the quantity of accumulated polymer. During the development of the models, it was necessary to add an inhibition constant on HB and HV consumption rates. As PHA is used as a carbon source by the cell at the end of the culture, it could be hypothesized that as long as another carbon source is available, there was no need for the cell to accelerate PHA consumption. In addition, when depolymerized, HB is oxidized in acetyl-CoA, while HV oxidation results in acetyl-CoA and propionyl-CoA. The PHA consumption rate might therefore also be limited by product inhibition, when those two molecules are present in the cell. This would explain why better fitting and parameter estimation were obtained when the same rate was applied to PHA and VFA consumptions. The maximal rates of those two phenomenons may be both limited by the availability of acetyl-CoA and propionyl-CoA. This kinetic structure allowed to obtain an accurate description of PHA production and consumption regardless of PHA composition and VFA mixture composition.

### 4.4. Impact of substrate on PHA composition

A direct relation between the carbon source used to support the growth of the bacteria and the PHA produced was demonstrated and extensively described. While acetate and butyrate lead to the production of HB, propionate and valerate produced a copolymer with high HV content (Bayon-Vicente et al., 2020b; Cabecas Segura et al., 2021; De Meur et al., 2020). When one of the latter is present in the mixture used as a carbon source, the polymer obtain is P(HB-co-HV). The proportion of each monomer depends on the concentration of propionate or valerate in the initial mix. A polymer with almost only HV was even obtained when propionate and valerate were used simultaneously as carbon source, which was never described so far. The yield of VFA conversion in HB and HV, used in the proposed mathematical models, shows the same tendency. Indeed, the yield of HV production is more important in culture using mixture of propionate and valerate as mixed carbon sources. It must also be noted that the presence of valerate in the mixture leads to a drastic increase of the HV conversion yield compared to propionate. In the prospect of PHA production, the composition of the initial substrate will therefore be a crucial point to obtain a polymer with the desired monomer composition. A valorization of waste stream via a two-step process might therefore be required to limit the variability of the substrate (Alloul et al., 2019). In addition, the fermentation effluent is typically composed in majority of acetate and butyrate, and the small concentrations of propionate and valerate in the effluent may therefore lead to PHA with a small proportion of HV in the polymer chain.

The sequential assimilations observed in some VFA mixtures may also impact polymer composition. For instance, in the case where acetate and valerate or butyrate and valerate are used as carbon source, even if the proportions of each monomer are the same, the profiles of monomer productions are very different and will lead to polymer with a different monomer arrangement.

## 5. Conclusion

In this study, macroscopic mechanistic models were developed to describe the production of PHA by *Rs. rubrum* when up to 4 different VFAs (acetate, propionate, butyrate, and valerate) are used as carbon sources. The resulting identified stoichiometric and kinetic parameters can be used to predict VFA consumption and PHA production during biomass growth. The good predictive capability of the proposed models and the related parameter accuracy, independently of the VFA mixture contents and polymer compositions, are quite encouraging and these satisfactory results, therefore, open the door to a better understanding and a more efficient production of PHA by *Rs. rubrum* growing on VFAs in industrial contexts. These mechanistic models are also promising candidates in view of model-based control applications.

## CRediT authorship contribution statement

**Paloma Cabecas Segura:** Data curation, Formal analysis, Investigation, Writing – original draft. **Ruddy Wattiez:** Funding acquisition, Resources, Writing – review & editing. **Vande Wouwer Alain:** Methodology, Resources, Software, Writing – review & editing. **Baptiste Leroy:** Funding acquisition, Conceptualization, Project administration, Supervision, Validation, Writing – review & editing. **Laurent Dewasme:** Data curation, Formal analysis, Investigation, Conceptualization, Supervision, Validation, Writing – original draft.

## Funding source

This work was supported by the Belgian Fund for Scientific Research (Grand Equipment-F.R.S-FNRS); the Concerted Research Action ARC Project [P. Cabecas, PHASYN, 2017]; the CDR-FNRS [B. Leroy, Redox homeostasis in purple bacteria].

## Declaration of Competing Interest

The authors declare that they have no known competing financial interests or personal relationships that could have appeared to influence

the work reported in this paper.

## Data Availability

Data will be made available on request.

## Appendix A. Supporting information

Supplementary data associated with this article can be found in the online version at doi:10.1016/j.jbiotec.2022.10.014.

## References


Alloul, A., Blansaer, N., Segura, P.C., Wattiez, R., Vlaeminck, S.E., Leroy, B., 2022. Dehazing redox homeostasis to foster purple bacteria biotechnology. Trends Biotechnol.

Alloul, A., Wuyts, S., Lebeer, S., Vlaeminck, S.E., 2019. Volatile fatty acids impacting phototrophic growth kinetics of purple bacteria: paving the way for protein production on fermented wastewater. Water Res 152, 138–147. https://doi.org/10.1016/j.watres.2018.12.025.

Bayon-Vicente, G., Marchand, E., Ducrotois, J., Dufrasne, F.E., Hallez, R., Wattiez, R., Leroy, B., 2021. Analysis of the involvement of the isoleucine biosynthesis pathway in photoheterotrophic metabolism of Rhodospirillum rubrum. Front. Microbiol. 0, 2721. https://doi.org/10.3389/FMICB.2021.731976.

Bayon-Vicente, G., Wattiez, R., Leroy, B., 2020a. Global proteomic analysis reveals high light intensity adaptation strategies and polyhydroxyalkanoate production in Rhodospirillum rubrum cultivated with acetate as carbon source. Front. Microbiol. 11, 1–17. https://doi.org/10.3389/fmicb.2020.00464.

Bayon-Vicente, G., Zarbo, S., Deutschbauer, A., Wattiez, R., Leroy, B., 2020b. Photoheterotrophic assimilation of valerate and associated polyhydroxyalkanoate production by Rhodospirillum rubrum. Appl. Environ. Microbiol. 86.

Beun, J.J., Dircks, K., Van Loosdrecht, M.C.M., Heijnen, J.J., 2002. Poly-β-hydroxybutyrate metabolism in dynamically fed mixed microbial cultures. Water Res. 36, 1167–1180.

Brandl, H., Gross, R.A., Lenz, R.W., Lloyd, R., Fuller, R.C., 1991. The accumulation of poly(3-hydroxyalkanoates) in Rhodobacter sphaeroides. Arch. Microbiol. 155, 337–340. https://doi.org/10.1007/bf00243452.

Brandl, H., Knee, E.J., Fuller, R.C., Gross, R.A., Lenz, R.W., 1989. Ability of the phototrophic bacterium Rhodospirillum rubrum to produce various poly (β-hydroxyalkanoates): potential sources for biodegradable polyesters. Int. J. Biol. Macromol. 11, 49–55. https://doi.org/10.1016/0141-8130(89)90040-8.

Cabecas Segura, Paloma, De Meur, Q., Alloul, A., Tanghe, A., Onderwater, R., Vlaeminck, S.E., Vande Wouwer, A., Wattiez, R., Dewasme, L., Leroy, B., 2022a. Preferential photoassimilation of volatile fatty acids by purple non-sulfur bacteria: experimental kinetics and dynamic modelling. Biochem. Eng. J.

Cabecas Segura, P., De Meur, Q., Tanghe, A., Onderwater, R., Dewasme, L., Wattiez, R., Leroy, B., 2021. Effects of mixing volatile fatty acids as carbon sources on Rhodospirillum rubrum carbon metabolism and redox balance mechanisms. Microorganisms 9 (9), 1996. https://doi.org/10.3390/microorganisms9091996.

Cabecas Segura, Paloma, Onderwater, R., Deutschbauer, A., Dewasme, L., Wattiez, R., Leroy, B., 2022b. Study of the production of poly (hydroxybutyrate-co-hydroxyhexanoate) and poly (hydroxybutyrate-co-hydroxyvalerate-co-hydroxyhexanoate) in Rhodospirillum rubrum. Appl. Environ. Microbiol. 88 (e01586-21).

Dahiya, S., Sarkar, O., Swamy, Y.V., Mohan, S.V., 2015. Acidogenic fermentation of food waste for volatile fatty acid production with co-generation of biohydrogen. Bioresour. Technol. 182, 103–113.

Dias, J.M.L., Oehmen, A., Serafim, L.S., Lemos, P.C., Reis, M.A.M., Oliveira, R., 2008. Metabolic modelling of polyhydroxyalkanoate copolymers production by mixed microbial cultures. BMC Syst. Biol. 2, 59.

Dias, J.M.L., Serafim, L.S., Lemos, P.C., Reis, M.A.M., Oliveira, R., 2005. Mathematical modelling of a mixed culture cultivation process for the production of polyhydroxybutyrate. Biotechnol. Bioeng. 92, 209–222.

Doi, Y., Kitamura, S., Abe, H., 1995. Microbial synthesis and characterization of poly(3-hydroxybutyrate-co-3-hydroxyhexanoate. Macromolecules 28, 4822–4828. https://doi.org/10.1021/ma00118a007.

Fradinho, J.C., Oehmen, A., Reis, M.A.M.M., 2014. Photosynthetic mixed culture polyhydroxyalkanoate (PHA) production from individual and mixed volatile fatty acids (VFAs): substrate preferences and co-substrate uptake. J. Biotechnol. 185, 19–27. https://doi.org/10.1016/j.jbiotec.2014.05.035.

Gopi, S., Kontopoulou, M., Ramsay, B.A., Ramsay, J.A., 2018. Manipulating the structure of medium-chain-length polyhydroxyalkanoate (MCL-PHA) to enhance thermal properties and crystallization kinetics. Int. J. Biol. Macromol. 119, 1248–1255.

Hustede, E., Steinbüchel, A., Schlegel, H.G., 1993. Relationship between the photoproduction of hydrogen and the accumulation of PHB in non-sulphur purple bacteria. Appl. Microbiol. Biotechnol. 39, 87–93.

Jiang, Y., Hebly, M., Kleerebezem, R., Muyzer, G., van Loosdrecht, M.C.M., 2011. Metabolic modeling of mixed substrate uptake for polyhydroxyalkanoate (PHA) production. Water Res. 45, 1309–1321. https://doi.org/10.1016/j.watres.2010.10.009.

Jiang, J., Zhang, Y., Li, K., Wang, Q., Gong, C., Li, M., 2013. Volatile fatty acids production from food waste: effects of pH, temperature, and organic loading rate. Bioresour. Technol. 143, 525–530. https://doi.org/10.1016/j.biortech.2013.06.025.

Kale, S.K., Deshmukh, A.G., Dudhare, M.S., Patil, V.B., 2015. Microbial degradation of plastic: a review. J. Biochem. Technol. 6, 952–961.

Keskin, G., Kızıl, G., Bechelany, M., Pochat-Bohatier, C., Öner, M., 2017. Potential of polyhydroxyalkanoate (PHA) polymers family as substitutes of petroleum based polymers for packaging applications and solutions brought by their composites to form barrier materials. Pure Appl. Chem. 89, 1841–1848.

Kitadokoro, K., Thumarat, U., Nakamura, R., Nishimura, K., Karatani, H., Suzuki, H., Kawai, F., 2012. Crystal structure of cutinase Est119 from Thermobifida alba AHK119 that can degrade modified polyethylene terephthalate at 1.76 Å resolution. Polym. Degrad. Stab. 97, 771–775.

Komemoto, K., Lim, Y.G., Nagao, N., Onoue, Y., Niwa, C., Toda, T., 2009. Effect of temperature on VFA's and biogas production in anaerobic solubilization of food waste. Waste Manag. 29, 2950–2955.

Lawrence, A.G., Schoenheit, J., He, A., Tian, J., Liu, P., Stubbe, J., Sinskey, A.J., 2005. Transcriptional analysis of Ralstonia eutropha genes related to poly-(R)-3-hydroxybutyrate homeostasis during batch fermentation. Appl. Microbiol. Biotechnol. 68, 663–672.

Lee, W.S., Chua, A.S.M., Yeoh, H.K., Ngoh, G.C., 2014. A review of the production and applications of waste-derived volatile fatty acids. Chem. Eng. J. 235, 83–99.

Leroy, B., De Meur, Q., Moulin, C., Wegria, G., Wattiez, R., 2015. New insight into the photoheterotrophic growth of the isocytrate lyase-lacking purple bacterium Rhodospirillum rubrum on acetate. Microbiology 161, 1061–1072. https://doi.org/10.1099/mic.0.000067.

Lim, S.-J., Kim, B.J., Jeong, C.-M., Ahn, Y.H., Chang, H.N., 2008. Anaerobic organic acid production of food waste in once-a-day feeding and drawing-off bioreactor. Bioresour. Technol. 99, 7866–7874.

McCully, A.L., Onyeziri, M.C., LaSarre, B., Gliessman, J.R., McKinlay, J.B., 2019. The reverse TCA cycle and reductive amino acid synthesis pathways contribute to electron balance in a Rhodospirillum rubrum Calvin cycle mutant. bioRxiv, 614065.

De Meur, Q., Deutschbauer, A., Koch, M., Bayon-Vicente, G., Cabecas Segura, P., Wattiez, R., Leroy, B., 2020. New perspectives on butyrate assimilation in Rhodospirillum rubrum S1H under photoheterotrophic conditions. BMC Microbiol. 1–20.

De Meur, Q., Wattier, R., 2017. Unravelling the volatile fatty acids assimilation in the MELiSSA loop. Proteomics Microbiol. University of Mons.

Narancic, T., Scollica, E., Kenny, S.T., Gibbons, H., Carr, E., Brennan, L., Cagney, G., Wynne, K., Murphy, C., Raberg, M., 2016. Understanding the physiological roles of polyhydroxybutyrate (PHB) in Rhodospirillum rubrum S1 under aerobic chemoheterotrophic conditions. Appl. Microbiol. Biotechnol. 100, 8901–8912.

Pardelha, F., Albuquerque, M.G.E., Reis, M.A.M., Dias, J.M.L., Oliveira, R., 2012. Flux balance analysis of mixed microbial cultures: application to the production of polyhydroxyalkanoates from complex mixtures of volatile fatty acids. J. Biotechnol. 162, 336–345.

Penloglou, G., Chatzidoukas, C., Kiparissides, C., 2012. Microbial production of polyhydroxybutyrate with tailor-made properties: an integrated modelling approach and experimental validation. Biotechnol. Adv. 30, 329–337. https://doi.org/10.1016/j.biotechadv.2011.06.021.

Salehizadeh, H., Van Loosdrecht, M.C.M., 2004. Production of polyhydroxyalkanoates by mixed culture: recent trends and biotechnological importance. Biotechnol. Adv. 22, 261–279.

Segers, L., Verstraete, W., 1983. Conversion of organic acids to H2 by Rhodospirillaceae grown with glutamate or dinitrogen as nitrogen source. Biotechnol. Bioeng. 25, 2843–2853.

Shang, L., Jiang, M., Chang, H.N., 2003. Poly (3-hydroxybutyrate) synthesis in fed-batch culture of Ralstonia eutropha with phosphate limitation under different glucose concentrations. Biotechnol. Lett. 25, 1415–1419.

Snell, K.D., Feng, F., Zhong, L., Martin, D., Madison, L.L., 2002. YfcX enables medium-chain-length poly (3-hydroxyalkanoate) formation from fatty acids in recombinant Escherichia coli fadB strains. J. Bacteriol. 184, 5696–5705.

Suhaimi, M., Liessens, J., Verstraete, W., 1987. $NH^{+}$/4–N assimilation by Rhodobacter capsulatus ATCC 23782 grown axenically and non-axenically in N and C rich media. J. Appl. Bacteriol. 62, 53–64.

Taidi, B., Mansfield, D.A., Anderson, A.J., 1995. Turnover of poly (3-hydroxybutyrate) (PHB) and its influence on the molecular mass of the polymer accumulated by Alcaligenes eutrophus during batch culture. FEMS Microbiol. Lett. 129, 201–205.

Tamis, J., Marang, L., Jiang, Y., van Loosdrecht, M.C.M., Kleerebezem, R., 2014. Modeling PHA-producing microbial enrichment cultures—towards a generalized model with predictive power. New Biotechnol. 31, 324–334.

Third, K.A., Newland, M., Cord-Ruwisch, R., 2003. The effect of dissolved oxygen on PHB accumulation in activated sludge cultures. Biotechnol. Bioeng. 82, 238–250.

Van Aalst-van Leeuwen, M.A., Pot, M.A., Van Loosdrecht, M.C.M., Heijnen, J.J., 1997. Kinetic modeling of poly (β-hydroxybutyrate) production and consumption by Paracoccus pantotrophus under dynamic substrate supply. Biotechnol. Bioeng. 55, 773–782.

Verlinden, R.A.J., Hill, D.J., Kenward, M.A., Williams, C.D., Radecka, I., 2007. Bacterial synthesis of biodegradable polyhydroxyalkanoates. J. Appl. Microbiol. 102, 1437–1449.

Wang, X., Carvalho, G., Reis, M.A.M., Oehmen, A., 2018. Metabolic modeling of the substrate competition among multiple VFAs for PHA production by mixed microbial cultures. J. Biotechnol. 280, 62–69.

Zhang, P., Chen, Y., Zhou, Q., 2009. Waste activated sludge hydrolysis and short-chain fatty acids accumulation under mesophilic and thermophilic conditions: effect of pH. Water Res. 43, 3735–3742.